Supplemental Figures

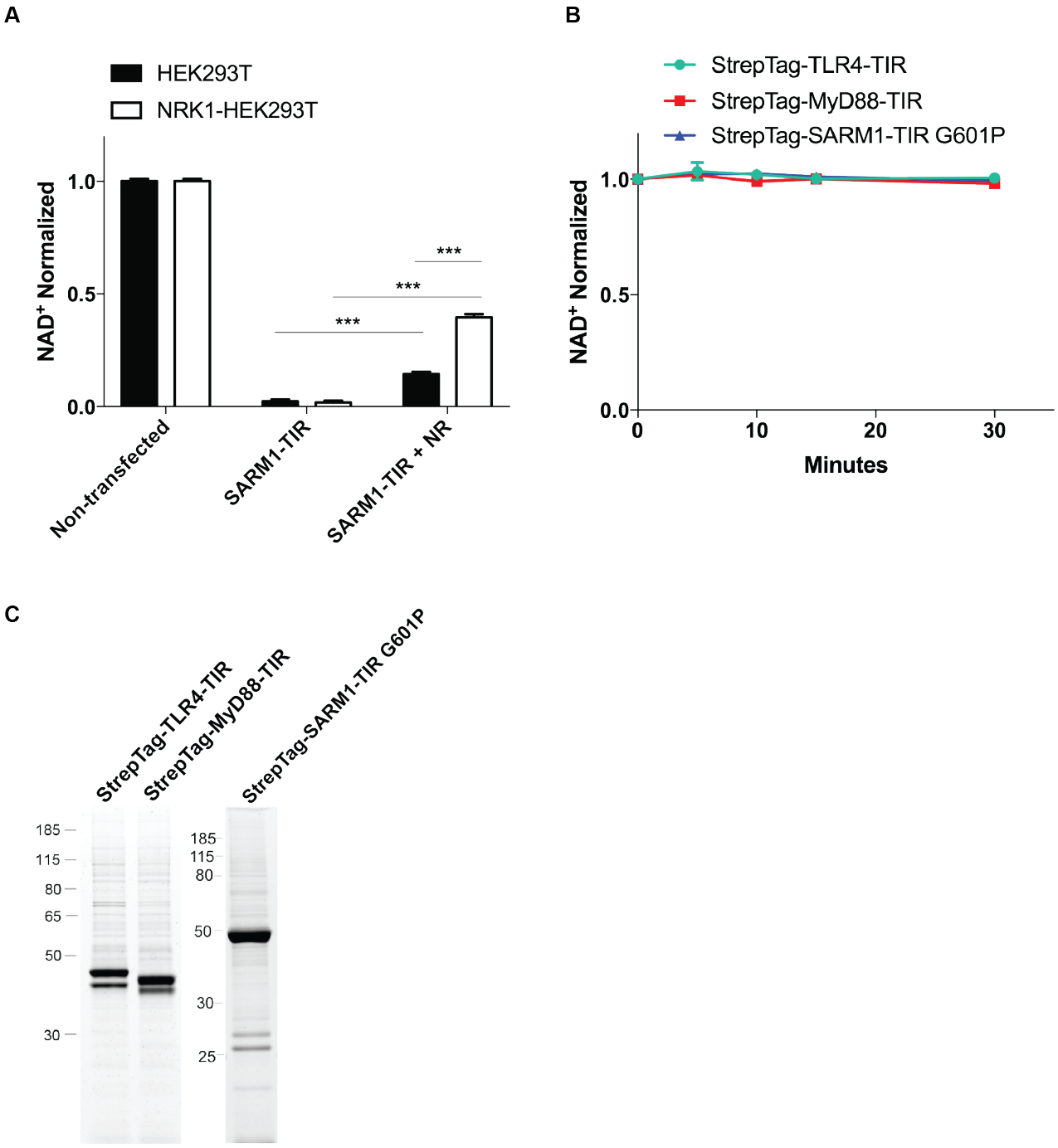

Figure S1: Purification of TIR domain complexes from NRK1-HEK293T cells (Related to Figure 1)
A) NRK1-HEK293T stable line with NR supplementation maintains higher NAD^+ levels than HEK293T with NR, upon SARM1-TIR expression. Data was generated from three independent NAD^+ measurements from three independent transfection experiments, and normalized to data from a non-transfected experiment run concurrently. **B**) NAD^+ reaction timecourse of human SARM1-TIR G601P, TLR4-TIR, and MyD88-TIR laden beads in in-vitro NADase assay (normalized to control at 0 min). **C**) Representative SYPRO Ruby gel of SARM1-TIR G601P, TLR4-TIR, and MyD88-TIR laden beads used in assay. Data for each time point was generated from three independent reaction experiments using purified protein from three independent transfection experiments. Data are presented as mean ± SEM; Error bars: SEM; *** $P < 0.001$ two tailed Student's t-test.

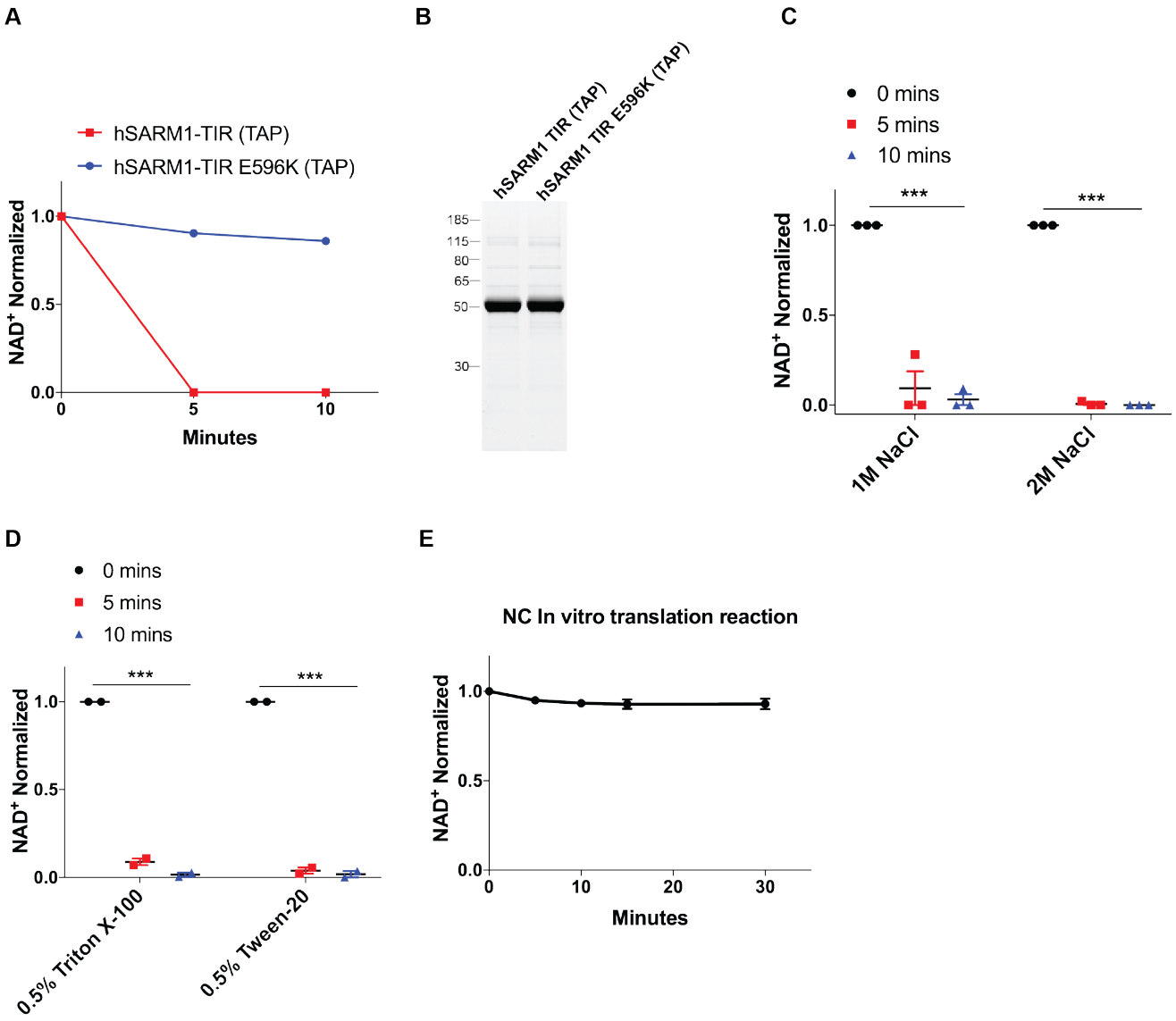

Figure S2: SARM1-TIR maintains NAD$^+$ cleavage activity after multiple purification schemes from mammalian cells and bacteria. (Related to Figure 2). **A**) Timecourse of NAD$^+$ cleavage reaction using tandem affinity purified (TAP) human SARM1-TIR (wild type and mutant) complexes expressed in mammalian cells (normalized to control at 0 min). **B**) SYPRO Ruby gel of TAP complexes used in assay; representative of three independent experiments. **C**) Timecourse of NAD$^+$ cleavage reaction using bacterially synthesized human SARM1-TIR, purified by TAP, and subjected to 1M and 2M NaCl washes during purification (normalized to control at 0 min). **D**) Timecourse of NAD$^+$ cleavage reaction using bacterially synthesized human SARM1-TIR, purified by TAP, and subjected to either 0.5% Triton X-100 or 0.5% Tween-20 washes during purification (normalized to control at 0 min) Data was generated from two independent reaction experiments and is represented as mean ± SEM. **E**) Reaction timecourse of purified components of the cell-free protein transcription/translation system incubated with NAD$^+$ and non-recombinant plasmid. Data for each time point in **A, C, E** was generated from three independent reaction experiments. Data are presented as mean ± SEM; Error bars: SEM. *** $P < 0.001$ one-way ANOVA.

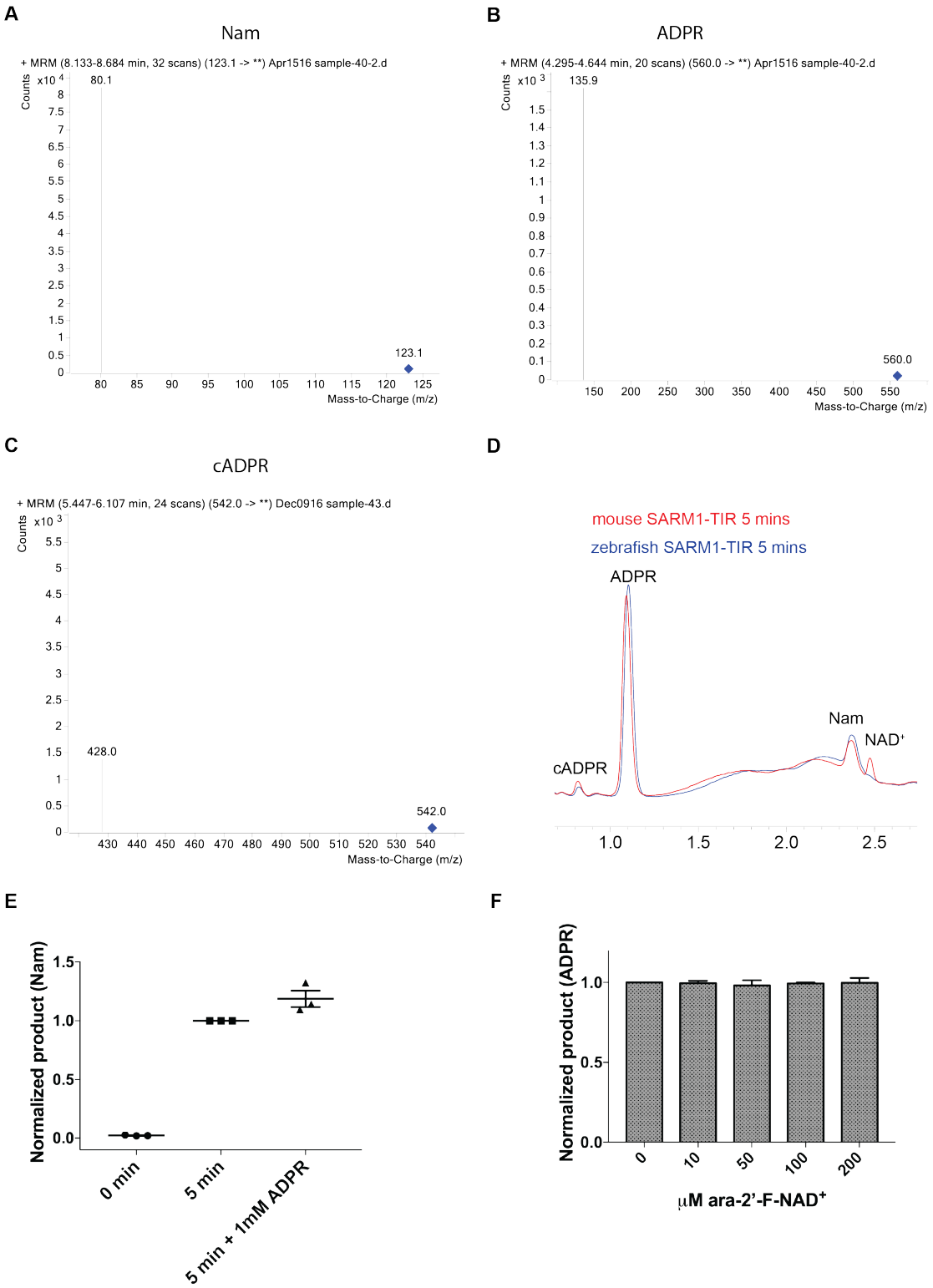

Figure S3: LC-MS/MS profiles of SARM1-TIR NAD$^+$ cleavage reaction products and effect of candidate NAD$^+$ analogs on enzymatic reaction (Related to Figure 3). **A-C**) LC-MS/MS spectra of Nam, cADPR, and ADPR from SARM1-TIR NAD$^+$ cleavage reaction. **D**) HPLC chromatograms showing mouse and zebrafish SARM1-TIR NAD$^+$ cleavage reaction generate Nam and ADPR as major products, and cADPR as a minor product. **E**) ADPR does not inhibit SARM1-TIR NADase activity (normalized to Nam generated at 5 min). **F**) ara-2'-F-NAD$^+$ does not inhibit SARM1-TIR NADase activity at doses as high as 40 fold the starting concentration of reaction NAD$^+$ (5µM). Metabolites were measured by HPLC after 5 minutes of reaction time.

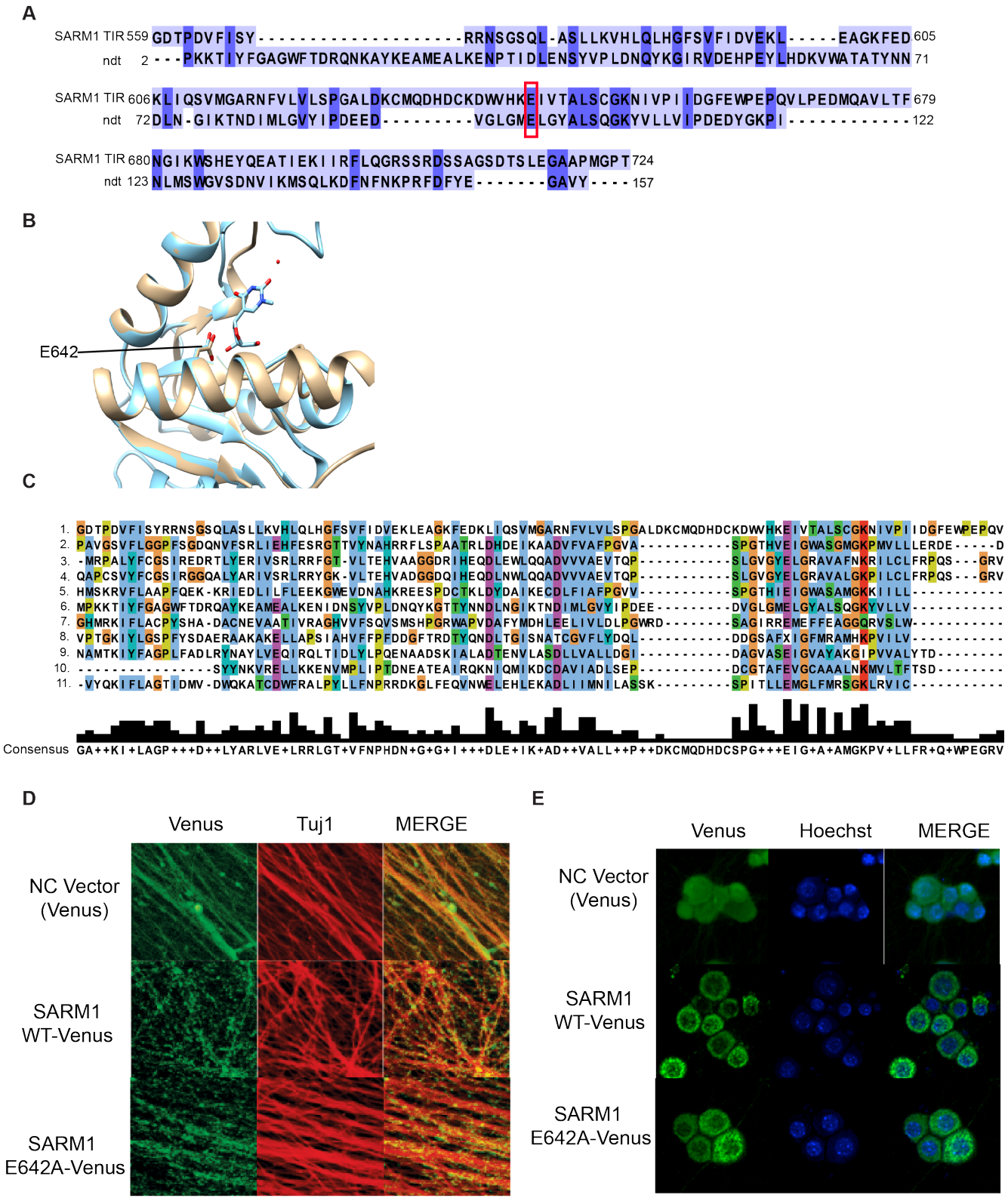

Figure S4: Structural modeling, sequence alignments with SARM1-TIR, and expression of SARM1-Venus constructs in SARM1-deficient DRGs (Related to Figure 4). **A**) Primary amino acid sequence alignment of SARM1-TIR with ndt (nucleoside 2-deoxyribosyltransferase) (PDB:1F8Y). Nucleoside 2-deoxyribosyltransferase catalytic glutamic acid is highlighted in red box and aligns to glutamic acid 642 in the SARM1-TIR domain. **B**) Modeling of the SARM1-TIR domain on the crystal structure of Nucleoside 2-deoxyribosyltransferase complexed with 5-Methyl-2'-deoxypseudouridine. E642 closely aligns with the catalytic residue of Nucleoside 2-deoxyribosyltransferase in the active site. **C**) Primary amino

acid sequence alignment of SARM1-TIR with candidate enzymes identified from HH pred based analysis (see Table S2). 1. SARM1-TIR 2. MilB CMP hydrolase 3. 2'-deoxynucleoside 5'-monophosphate N-hydrolase 1 4. 2'-deoxyribonucleoside 5'-monophosphate N-glycosidase 5. BcmB CMP glycosidase 6. Nucleoside 2-deoxyribsoyltranferase 7. Uncharacterized protein (P. aeruginosa) 8. Purine 2'-deoxyribosyltransferase 9. uncharacterized protein (E.faecalis) 10. nucleoside 2'-deoxyribosyltransferase 11. nucleoside deoxyribosyltransferase. **D)** Venus expression of indicated constructs in DRG axons, co-stained for Tuj1 to assess total axon area for each field. **E**) Venus expression of indicated constructs in DRG cell bodies, co-stained with Hoechst to assess total nuclei in each field.

Table S2: **Nucleotide hydrolase/transferase enzymes identified via HHPred** (**Related to Figure 4 and S4**). SARM1-TIR was used as a query sequence in HHPred to identify candidate enzymes.

PDB	Protein Identification	Probability	E-value	P-value
4jem	cytidine 5' monophosphate hydrolase MilB	98.5	1.70E-06	4.50E-11
2khz	2'-deoxyribonucleoside 5'-monophosphate N-glycosidase	98.3	1.40E-05	3.70E-10
4p5e	2'-deoxynucleoside 5'-phosphate N-hydrolase 1	98.2	1.40E-05	3.70E-10
4jen	cytidine 5' monophosphate N-glycosidase BcmB	98.2	4.90E-06	1.30E-10
1s2d	purine 2'-deoxyribosyltransferase	97.9	0.00011	2.90E-09
1t1j	Uncharacterized protein from P aeruginosa	97.6	0.0002	5.30E-09
1f8y	Nucleoside 2-deoxyribosyltransferase	97.6	0.00021	5.50E-09
3ehd	Uncharacterized conserved protein from E. faecalis	97.6	0.00039	1.00E-08
2f62	Nucleoside 2-deoxyribosyltransferase	97.4	0.0016	4.10E-08
4mcj	putative nucleoside deoxyribosyltransferase	97.1	0.0023	5.90E-08